Landscape statistics of the p-spin Ising model

Viviane M de Oliveira and J F Fontanari
Instituto de Física de São Carlos
Universidade de São Paulo
Caixa Postal 369
13560-970 São Carlos SP
Brazil

Abstract

The statistical properties of the local optima (metastable states) of the infinite range Ising spin glass with p-spin interactions in the presence of an external magnetic field h are investigated analytically. The average number of optima as well as the typical overlap between pairs of identical optima are calculated for general p. Similarly to the thermodynamic order parameter, for $p > 2$ and small h the typical overlap q_t is a discontinuous function of the energy. The size of the jump in q_t increases with p and decreases with h, vanishing at finite values of the magnetic field.

Short Title: landscape of the p-spin model
PACS: 05.50+q, 87.10+e, 64.60Cn

1 Introduction

The emphasis professed by Kauffman on the role of the topology of the fitness landscape as a source of order in contraposition to natural selection has arisen considerable interest in the study of the statistical properties of fitness landscapes [1]. The central issue is the limitation imposed by the structure of the fitness landscapes on adaptive evolution, viewed as a local hill-climbing procedure via fitter mutants. (See [2] for a lucid criticism of these ideas.) For sake of concreteness, let us consider a population of asexually reproducing haploid organisms whose genotypes are described by sequences of N Ising spins $\mathbf{s} = (s_1, \ldots, s_N)$ with $s_i = \pm 1$. In the discrete space of the 2^N possible sequences, evolution is modelled by an adaptive walk defined as a connected walk through a succession of neighboring sequences (i.e., sequences that differ by a single spin only) each of which possessing improved fitness [1]. There are several questions of interest whose answers may shed light on the structure of the landscapes as, for instance, the number of fitness optima in the sequence space and the similarity between these optima, to mention only those we will address in this paper.

Most of the analyses have concentrated on the NK model of random epistatic interactions since it possesses a tunable control parameter that regulates the ruggedness of the fitness landscape [1, 3, 4]. An alternative (and more appealing to the physicists) class of fitness functions was proposed by Amitrano *et al.* [5], namely, the Ising spin glass with p-spin interactions defined by the random energy function [6, 7]

$$\mathcal{H}_p(\mathbf{s}) = -\sum_{1 \le i_1 < i_2 \ldots < i_p \le N} J_{i_1 i_2 \ldots i_p} s_{i_1} s_{i_2} \ldots s_{i_p} - h \sum_i s_i \tag{1}$$

where the coupling strengths are statistically independent random variables with a Gaussian distribution

$$\mathcal{P}\left(J_{i_1 i_2 \ldots i_p}\right) = \sqrt{\frac{N^{p-1}}{\pi p!}} \exp\left[-\frac{\left(J_{i_1 i_2 \ldots i_p}\right)^2 N^{p-1}}{p!}\right], \tag{2}$$

and h is the external magnetic field. In this context the fitness value ascribed to a sequence or genotype $\mathbf{s}$ is the reverse of its energy. Thus the fitness maxima correspond to the energy minima of (1). Henceforth we will refer to the fitness maxima or energy minima as simply optima. For $p = 1$ or $h \to \infty$ the energy (1) gives a single-peaked, smooth correlated landscape, while the limit $p \to \infty$ corresponds to the random energy model of Derrida [6] and yields an extremely rugged, uncorrelated landscape. The case $p = 2$ is the well-known SK model [8], which exhibits a large number of highly correlated local optima [9, 10].

For general p, little is known about the statistical features of the landscape generated by the energy function (1). A result worth mentioning is that, for $h = 0$, the correlation between values of $\mathcal{H}_p$ for different configurations is given by [5, 11]

$$\left\langle \mathcal{H}_p\left(\mathbf{s}^a\right) \mathcal{H}_p\left(\mathbf{s}^b\right) \right\rangle = \left[q\left(\mathbf{s}^a, \mathbf{s}^b\right)\right]^p \tag{3}$$

where

$$q\left(\mathbf{s}^a, \mathbf{s}^b\right) = \frac{1}{N}\sum_{i=1}^{N} s_i^a s_i^b \tag{4}$$

is the overlap between the two arbitrary states $\mathbf{s}^a$ and $\mathbf{s}^b$. Here the average indicated by $\langle \ldots \rangle$ is taken over the probability distribution of the couplings (2). Thus, as mentioned before, the correlations between energy levels vanish for $p \to \infty$.

The thermodynamics of the p-spin Ising model has been investigated within the replica framework [7, 12, 13]. In particular, for $p = 2$ the order parameter function $q(x)$ tends to zero continuously as the temperature approaches a critical value at which the transition between the spin glass and the high temperature (disordered) phases takes place [9, 10]. For $p \to \infty$, the system has a critical temperature T_c at which it freezes completely into the ground state: $q(x)$ is a step function with values zero and one, and with a break point at $x = T/T_c$ [7]. The situation for finite $p > 2$ is considerably more complicated. There is a transition from the disordered phase to a partially frozen phase characterized by a step function $q(x)$ with values zero and $q_1 < 1$. As the temperature is lowered further, a second transition occurs, leading to a phase described by a continuous order parameter function [12, 13].

The goal of this paper is to investigate the statistical properties of the fixed points (local or global optima) of adaptive walks on the fitness landscape defined by equation (1). The energy cost of flipping the spin s_i is $\delta\mathcal{H}_p = 2\Delta_i$ where

$$\Delta_i = \sum_{i_2 < \ldots < i_p} J_{i i_2 \ldots i_p}\, s_i s_{i_2} \ldots s_{i_p} + h s_i. \tag{5}$$

is termed the stability of s_i. Since in an adaptive walk only flippings or moves that decrease the energy (i.e., increase the fitness) are allowed, any state $\mathbf{s}$ that satisfies

$$\Delta_i > 0 \qquad \forall i \tag{6}$$

is an optima of the fitness landscape. Clearly, counting the number of states that obey (6) is equivalent to calculating the number of solutions of the zero-temperature limit of the celebrated TAP equations [14]. For non-zero temperature, the quite involved calculation of the average number of solutions of the TAP equations has been carried out for $p = 2$ [15] as well as for general p [16]. However, systematic analyses of the typical energy of the local optima and of the effects of the external magnetic field have been undertaken for the simplest case only, namely, $p = 2$ at zero temperature [17, 18, 19]. We note that in the statistical mechanics context the local optima are usually termed metastable states.

In this paper we study at length the effects of the magnetic field h on the structure of the local optima of the p-spin energy landscape. More pointedly, we calculate analytically the average number of local optima with a fixed energy density ϵ, denoted by $\langle \mathcal{N}(\epsilon) \rangle$. Although this analysis is quite straighforward, it is justified since the dependence of that quantity on ϵ and h has not been investigated for general p. In fact, we note that results of extensive numerical simulations aimed at

measuring $\langle \mathcal{N}(\epsilon)$ have been reported recently [20]. More importantly, we calculate the average number of pairs of local optima with overlap q and fixed energy density ϵ. This quantity, denoted by $\langle \mathcal{M}(q,\epsilon)\rangle$, allows us to determine the typical overlap q_t between pairs of local optima with energy density ϵ. Since $\langle \mathcal{M}(q_t,\epsilon)\rangle$ is directly related to the second moment of $\mathcal{N}(\epsilon)$, we can determine the regions in the space of parameters (p,ϵ,h) where this random variable is self-averaging.

The remainder of the paper is organized as follows. In Sec. 2 we derive the formal equation for the nth moment of the random variable $\mathcal{N}(\epsilon)$. Then we use that result to calculate the average number of local optima $\langle \mathcal{N}(\epsilon)\rangle$ in Sec. 3, and the average number of pairs of local optima $\langle \mathcal{M}(q,\epsilon)\rangle$ in Sec. 4. Finally, some concluding remarks are presented in Sec. 5.

2 The formalism

The number of local optima $\mathcal{N}(\epsilon)$ with fixed energy density ϵ can be calculated by introducing the quantity $Y_{\mathbf{s}}$ defined by

$$Y_{\mathbf{s}} = \begin{cases} 1 & \text{if } \epsilon N = \mathcal{H}_p(\mathbf{s}) \text{ and } \Delta_i > 0 \ \ \forall i \\ 0 & \text{otherwise} \end{cases} , \tag{7}$$

so that

$$\mathcal{N}(\epsilon) = \mathrm{Tr}_{\mathbf{s}} Y_{\mathbf{s}}, \tag{8}$$

where $\mathrm{Tr}_{\mathbf{s}}$ denotes the summation over the 2^N states of the system. We are interested in the evaluation of the moment $\langle [\mathcal{N}(\epsilon)]^n \rangle$ for $n = 1, 2$, which can be written as

$$\begin{aligned} \langle [\mathcal{N}(\epsilon)]^n \rangle &= \left\langle \prod_{a=1}^{n} \mathrm{Tr}_{\mathbf{s}^a} Y_{\mathbf{s}^a} \right\rangle \\ &= \mathrm{Tr}_{\mathbf{s}^1} \ldots \mathrm{Tr}_{\mathbf{s}^n} \mathcal{W}\left(Y_{\mathbf{s}^1} = 1, \ldots, Y_{\mathbf{s}^n} = 1\right) \end{aligned} \tag{9}$$

where $\mathcal{W}\left(Y_{\mathbf{s}^1} = 1, \ldots, Y_{\mathbf{s}^n} = 1\right)$ is the joint probability that the n random variables $Y_{\mathbf{s}^1}, \ldots, Y_{\mathbf{s}^n}$ assume the value 1. Using the definition

$$\mathcal{W}\left(Y_{\mathbf{s}^1} = 1, \ldots, Y_{\mathbf{s}^n} = 1\right) = \left\langle \prod_{a=1}^{n} \delta\left[\epsilon - \mathcal{H}_p\left(\mathbf{s}^a\right)/N\right] \prod_i \Theta\left(\Delta_i^a\right) \right\rangle, \tag{10}$$

the equation for the nth moment becomes

$$\langle [\mathcal{N}(\epsilon)]^n \rangle = \left\langle \prod_{a=1}^{n} \mathrm{Tr}_{\mathbf{s}^a} \delta\left[\epsilon N - \mathcal{H}_p\left(\mathbf{s}^a\right)\right] \prod_i \Theta\left(\Delta_i^a\right) \right\rangle. \tag{11}$$

where $\Theta(x) = 1$ if $x > 0$ and 0 otherwise. We have presented the derivation of equation (11) in detail because some authors have written the random variable

$\mathcal{N}(\epsilon)$ in terms of the delta function directly [18, 19]. Clearly, this procedure is correct only for the moments of $\mathcal{N}(\epsilon)$ as shown above.

In the next two sections we concentrate on the explicit evaluation of equation (11) for $n = 1$ and 2. To facilitate those calculations, we express the energy $\mathcal{H}_p(\mathbf{s})$ in terms of the stabilities Δ_i,

$$\mathcal{H}_p(\mathbf{s}) = -\frac{1}{p}\sum_i \left(\Delta_i + h(p-1)s_i\right), \tag{12}$$

so that the dependence on the couplings in equation (11) appears only through the stabilities Δ_i.

3 Average number of optima

Using the integral representation of the delta function and the auxiliary relation (12) we can write the first moment of $\mathcal{N}(\epsilon)$ as

$$\begin{aligned}\langle\mathcal{N}(\epsilon)\rangle &= \int_{-\infty}^{\infty}\frac{d\tilde{\epsilon}}{2\pi}\exp\left(\mathbf{i}N\epsilon\tilde{\epsilon}\right)\prod_i\int_{-\infty}^{\infty}\frac{d\Delta_i d\tilde{\Delta}_i}{2\pi}\Theta\left(\Delta_i\right)\exp\left(\mathbf{i}\Delta_i\tilde{\Delta}_i\right)\\ &\times\mathrm{Tr}_{\mathbf{s}}\exp\left[-\mathbf{i}h\sum_i\tilde{\Delta}_i s_i + \frac{\mathbf{i}}{p}\tilde{\epsilon}\sum_i\left(\Delta_i + h(p-1)s_i\right)\right]\\ &\times\left\langle\exp\left(-\mathbf{i}\sum_i\tilde{\Delta}_i\sum_{i_2<\ldots<i_p}J_{ii_2\ldots i_p}s_i s_{i_2}\ldots s_{i_p}\right)\right\rangle.\end{aligned} \tag{13}$$

The average over the couplings can be easily carried out using the identity

$$\sum_i\tilde{\Delta}_i\sum_{i_2<\ldots<i_p}J_{ii_2\ldots i_p}s_i s_{i_2}\ldots s_{i_p} = \sum_{i_1<\ldots<i_p}\left(\sum_{k=1}^{p}\tilde{\Delta}_{i_k}\right)J_{i_1\ldots i_p}s_{i_1}\ldots s_{i_p} \tag{14}$$

and yields, in the limit $N\to\infty$,

$$\begin{aligned}\langle\ldots\rangle &= \exp\left[-\frac{p!}{4N^{p-1}}\sum_{i_1<\ldots<i_p}\left(\sum_{k=1}^{p}\tilde{\Delta}_{i_k}\right)^2\right]\\ &= \exp\left[-\frac{p}{4}\sum_i\left(\tilde{\Delta}_i\right)^2 - \frac{p(p-1)}{4N}\left(\sum_i\tilde{\Delta}_i\right)^2\right].\end{aligned} \tag{15}$$

The remaining calculations are straightforward: a Gaussian transformation allows us to decouple the sites in (15), so that the integrals over Δ_i and $\tilde{\Delta}_i$ as well as the trace over the spins can be readily performed. As usual, we conclude the calculation

by carrying out a saddle-point integration over two appropriately rescaled saddle-point parameters. The final result for the exponent f in $\langle \mathcal{N}(\epsilon) \rangle = \mathrm{e}^{Nf}$ is

$$\begin{aligned} f &= \frac{\epsilon\nu}{\sqrt{p}} - \frac{1}{p-1}\left(\mu^2 - \mu\nu + \frac{\nu^2}{4p}\right) - \ln 2 \\ &\quad + \ln\left[\mathrm{e}^{\bar{h}\nu}\mathrm{erfc}\left(-\mu - \bar{h}\right) + \mathrm{e}^{-\bar{h}\nu}\mathrm{erfc}\left(-\mu + \bar{h}\right)\right], \end{aligned} \tag{16}$$

where

$$\bar{h} = \frac{h}{\sqrt{p}}. \tag{17}$$

Here the saddle-point parameters ν and μ are obtained by solving the equations $\partial f/\partial\nu = 0$ and $\partial f/\partial\mu = 0$ simultaneously. In figure 1 we present the exponent f as a function of ϵ for $p = 2$ and several values of h. For sake of clarity we present only positive values of f. The decrease in the number of local optima as h increases indicates that the landscape becomes smoother, as expected. The results for $p > 2$ are qualitatively similar, except that the peaks are higher and slightly broader. Two values of the energy density are particularly important, namely, the value at which f reaches its maximum value f_t, denoted by ϵ_t, and the lowest value of ϵ for which f vanishes, denoted by ϵ_0. While ϵ_t gives the typical value of the energy density of the local optima, ϵ_0 gives a lower bound to the ground state energy density of the spin model defined by the hamiltonian (1) [17]. In figures 2 an 3 we present ϵ_t and f_t, respectively, as a function of h for several values of p. These quantities are easily obtained by setting $\nu = 0$ in equation (16). The single saddle-point equation $\partial f/\partial\mu = 0$ possesses either one root (for either small or large values of h) or three roots (for intermediate values of h). The discontinuity in ϵ_t that can be observed in figure 2 for $p \geq 7$ is due to the simultaneous disappearance of two of those roots. For $p \to \infty$ and finite h we find $\epsilon_t \to \langle \mathcal{H}_p \rangle = 0$, signaling thus the emergence of the so-called complexity catastrophe, i.e., the energy density of typical local optima equals the expected energy of a randomly chosen state [1]. We note that $\langle \mathcal{N}(\epsilon_t) \rangle = \exp(f_t N)$ yields the average number of optima regardless of their energy values, i.e., the same result is obtained by dropping the energy constraint in the definition of $Y_{\mathbf{s}}$ given in equation (7). In figure 4 we present ϵ_0 as a function of h for several values of p. Clearly, since in the limit $h \to \infty$ there is only one optimum, namely, $\mathbf{s} = \mathbf{1}$, we find $\epsilon_0 \to \epsilon_t = -h$. It is important to note that for $p \to \infty$, ϵ_0 tends to a non-zero limiting value. This result illustrates the fact that the complexity catastrophe phenomenon affects the typical optima only. In fact, the increase of p has little effect on the ground-state lower bound ϵ_0, which for $h = 0$ decreases from -0.791 for $p = 2$ [15] to $-\sqrt{\ln 2} \approx -0.832$ for $p \to \infty$ [6].

4 Average number of pairs of optima

We define the number of pairs of optima with overlap $q = -1, -1 + \frac{2}{N}, \ldots, 1$ and energy density ϵ as

$$\mathcal{M}(q,\epsilon) = \frac{1}{2}\mathrm{Tr}_{\mathbf{s}^1}\mathrm{Tr}_{\mathbf{s}^2} Y_{\mathbf{s}^1} Y_{\mathbf{s}^2} \delta\left(Nq, \sum_i s_i^1 s_i^2\right) \tag{18}$$

where $\delta(m,n)$ is the Kronecker delta and $Y_{\mathbf{s}}$ is given by equation (7). Following the procedure presented in Sec. 2, the average of $\mathcal{M}$ over the couplings is cast into the form

$$\langle \mathcal{M}(q,\epsilon)\rangle = \frac{1}{2}\left\langle \mathrm{Tr}_{\mathbf{s}^1}\mathrm{Tr}_{\mathbf{s}^2}\delta\left(Nq, \sum_i s_i^1 s_i^2\right)\prod_{a=1}^{2}\delta\left[\epsilon N - \mathcal{H}_p\left(\mathbf{s}^a\right)\right]\prod_i \Theta\left(\Delta_i^a\right)\right\rangle. \tag{19}$$

The integral representations of the delta function and the Kronecker delta allow us to write this equation as

$$\begin{aligned}
\langle \mathcal{M}(q,\epsilon)\rangle \;=\; & \frac{1}{2}\int_{-\pi}^{\pi}\frac{d\tilde{q}}{2\pi}\exp\left(\mathbf{i}Nq\tilde{q}\right)\prod_a\int_{-\infty}^{\infty}\frac{d\tilde{\epsilon}^a}{2\pi}\exp\left(\mathbf{i}N\epsilon^a\tilde{\epsilon}^a\right) \\
& \times\prod_{ai}\mathrm{Tr}_{\mathbf{s}^a}\int_{-\infty}^{\infty}\frac{d\Delta_i^a d\tilde{\Delta}_i^a}{2\pi}\Theta\left(\Delta_i^a\right)\exp\left(\mathbf{i}\Delta_i^a\tilde{\Delta}_i^a\right) \\
& \times\exp\left[-\mathbf{i}\tilde{q}\sum_i s_i^1 s_i^2 - \mathbf{i}h\sum_{ai}\tilde{\Delta}_i^a s_i^a + \frac{\mathbf{i}}{p}\sum_{ai}\tilde{\epsilon}^a\left(\Delta_i^a + h(p-1)s_i^a\right)\right] \\
& \times\left\langle\exp\left(-\mathbf{i}\sum_{ai}\tilde{\Delta}_i^a\sum_{i_2<\ldots<i_p}J_{ii_2\ldots i_p}s_i^a s_{i_2}^a\ldots s_{i_p}^a\right)\right\rangle.
\end{aligned} \tag{20}$$

As in the previous section, the average can be performed with the aid of an identity analogous to (14), yielding

$$\langle\ldots\rangle = \exp\left\{-\frac{p!}{4N^{p-1}}\sum_{i_1<\ldots<i_p}\left[\sum_{a=1}^{2}\left(\sum_{k=1}^{p}\tilde{\Delta}_{i_k}^a\right)s_{i_1}^a\ldots s_{i_p}^a\right]^2\right\}. \tag{21}$$

After some algebra, the argument of this exponential is rewritten in the limit $N\to\infty$ as

$$\begin{aligned}
\{\ldots\} \;=\; & -\frac{p}{4}\sum_{a=1}^{2}\left[\sum_i\left(\tilde{\Delta}_i^a\right)^2 + \frac{p-1}{N}\left(\sum_i\tilde{\Delta}_i^a\right)^2\right] - \frac{p\,q^{p-1}}{2}\sum_i\tilde{\Delta}_i^1\tilde{\Delta}_i^2 s_i^1 s_i^2 \\
& -\frac{p(p-1)\,q^{p-2}}{2N}\left(\sum_i\tilde{\Delta}_i^1 s_i^1 s_i^2\right)\left(\sum_i\tilde{\Delta}_i^2 s_i^1 s_i^2\right).
\end{aligned} \tag{22}$$

The next step is to introduce via delta functions the auxiliary parameters: $Nm_1 = \sum_i \tilde{\Delta}_i^1$, $Nm_2 = \sum_i \tilde{\Delta}_i^2$, $Nv_1 = \sum_i \tilde{\Delta}_i^1 s_i^1 s_i^2$, $Nv_2 = \sum_i \tilde{\Delta}_i^2 s_i^1 s_i^2$, and their respective Lagrange multipliers in order to decouple the variables s_i^a and $\tilde{\Delta}_i^a$ for different sites i. Then the integrals over Δ_i^a and $\tilde{\Delta}_i^a$, and the trace over s_i^a can be easily performed. As before, the auxiliary parameters as well as the Lagrange multipliers $\tilde{q}$ and $\tilde{\epsilon}$ are integrated out via a saddle-point integration. This part of the calculation is straightforward and quite unilluminating so we do not present any further detail. To proceed further we assume that the symmetry $\mathbf{s}^1 \leftrightarrow \mathbf{s}^2$ between the two replicas remains intact, i.e., $m_1 = m_2$ and $v_1 = v_2$. This is a quite sensible assumption since the breaking of the replica symmetry that pervades the thermodynamic calculations [7, 12, 13] is very probably a consequence of the limit where the number of replicas goes to zero. In any event we will, conservatively, restrict the forthcoming analysis to pairs of identical optima only. The final result for the exponent g in $\langle \mathcal{M}(q,\epsilon)\rangle = \frac{1}{2}\exp(gN)$ is written more simply in terms of a new set of saddle-point parameters that are linear combinations of those introduced above. We find

$$\begin{aligned} g &= \frac{\epsilon\nu}{\sqrt{p}} + qz - \frac{1}{2(p-1)}\left[(x+y)^2 + q^{2-p}\,(x-y)^2 + (1+q^p)\frac{\nu^2}{4p}\right] \\ &\quad + \frac{\nu}{2(p-1)}\left[(1+q)\,x + (1-q)\,y\right] + \ln\Xi\,(\nu,x,y,z) - \ln 2 \end{aligned} \tag{23}$$

where

$$\begin{aligned} \Xi &= \mathrm{e}^{\nu\bar{h}-z}\int_{-x-\bar{h}}^{\infty} Dt\,\mathrm{erfc}\left[-\frac{x+\bar{h}+q^{p-1}t}{\sqrt{1-q^{2p-2}}}\right] \\ &\quad + \mathrm{e}^{-\nu\bar{h}-z}\int_{-x+\bar{h}}^{\infty} Dt\,\mathrm{erfc}\left[-\frac{x-\bar{h}+q^{p-1}t}{\sqrt{1-q^{2p-2}}}\right] \\ &\quad + \mathrm{e}^{z}\int_{-y+\bar{h}}^{\infty} Dt\,\mathrm{erfc}\left[-\frac{y+\bar{h}-q^{p-1}t}{\sqrt{1-q^{2p-2}}}\right] \\ &\quad + \mathrm{e}^{z}\int_{-y-\bar{h}}^{\infty} Dt\,\mathrm{erfc}\left[-\frac{y-\bar{h}-q^{p-1}t}{\sqrt{1-q^{2p-2}}}\right]. \end{aligned} \tag{24}$$

Here $Dt = dt\mathrm{e}^{-t^2}/\sqrt{\pi}$ is the Gaussian measure and $\bar{h}$ is given by (17). The saddle-point parameters ν, x, y, z must be determined so as to maximize g. This is achieved by solving the four coupled saddle-point equations $\partial g/\partial\nu = 0$, $\partial g/\partial x = 0$, $\partial g/\partial y = 0$, and $\partial g/\partial z = 0$. For $q = 1$ we find $y = 0$ and hence $g = f$, as expected. Furthermore, for $q = 0$ and $h = 0$ we find $x = y$ and $z = 0$ so that $g = 2f$. Once $\langle \mathcal{M}(q,\epsilon)\rangle$ is known, the second moment of $\mathcal{N}(\epsilon)$ can be calculated using the identity

$$\begin{aligned} \sum_q \langle \mathcal{M}(q,\epsilon)\rangle &= \frac{1}{2}\langle[\mathcal{N}(\epsilon)]^2\rangle \\ &\approx \langle \mathcal{M}(q_t,\epsilon)\rangle, \end{aligned} \tag{25}$$

since the sum is dominated by the overlap $q = q_t$ that maximizes equation (23) in the limit $N \to \infty$. Hence we have $\langle [\mathcal{N}(\epsilon)]^2 \rangle = \exp\left(f^{(2)}N\right)$ with $f^{(2)}$ given by (23) calculated at q_t. Thus for $h = 0$ the variance of the random variable $\mathcal{N}(\epsilon)$ vanishes in the thermodynamic limit, provided that $q_t = 0$. We note that although $q = 0$ is always a point of maximum of g for $h = 0$, that maximum may not be the global one and, in that case, $q_t \neq 0$.

For fixed q, the dependence of g on ϵ is similar to that shown in figure 1. Likewise, the maximum of g with respect to ϵ, denoted by g_t, is determined by setting $\nu = 0$. In figure 5 we show this maximum as a function of q for $p = 7$ and several values of h. The quantity $\frac{1}{2}\exp(g_t N)$ can be viewed as the number of pairs of identical optima (in the sense that their energies and saddle-point parameters are identical) with overlap q, regardless of the specific value of their energies. For h not too large there appears a minimum for $q \approx 1$, indicating that around a typical optimum there is a region where other optima are rarer. The picture that emerges is one of clusters of many optima surrounded by comparatively smoother valleys. The typical energy ϵ_t of these optima is shown in figure 6 as a function of the overlap q. The typical overlap q_t between the optima increases from zero at $h = 0$ to one in the limit $h \to \infty$ since, as expected, the external magnetic field induces correlations between the optima. This is shown in figure 7, where we present q_t as a function of h for several values of p. The discontinuity that appears for $p \geq 7$ is caused by the competition between the two maxima shown in figure 5.

Next we consider the dependence of the typical overlap between identical optima on their energies. This analysis is more involved since, besides the four saddle-point equations, we have to solve the equation $\partial g/\partial q = 0$ too. In figures 8 and 9 we show q_t as a function of ϵ for $p = 2$ and $p = 3$, respectively, and several values of the external magnetic field. For $h = 0$, in both cases we find $q_t = 0$ up to a certain value of the energy density ($\epsilon = -0.672$ for $p = 2$ and $\epsilon = -0.792$ for $p = 3$). Thus, as mentioned before, $\mathcal{N}(\epsilon)$ is self-averaging in this regime. Our results for $p = 2$ are remarkably similar to those found in the replica calculation of the quenched average $\langle \ln \mathcal{N}(\epsilon) \rangle$, with the typical overlap q_t replaced by the saddle-point parameter $\hat{q} = \langle \langle s_i \rangle_\epsilon^2 \rangle$ [18]. Here $\langle \ldots \rangle_\epsilon$ means an average over optima with energy density ϵ. In particular, $\hat{q}$ vanishes for $\epsilon > -0.672$, indicating thus that $\mathcal{N}(\epsilon)$ is self-averaging in this regime, in agreement with our results. However, while for $p = 2$, q_t increases continuously from zero, for $p = 3$ there is a discontinuity at $\epsilon = -0.792$. The same phenomenon is observed for $p > 3$, with the size of the jump in q_t increasing with p. This finding is reminiscent of the jump in the order parameter found in the thermodynamic calculations for $p > 2$ [12, 13]. The discontinuity in q_t can be understood by studying the dependence of the exponent g on the overlap q for $p = 3$ and $h = 0$, shown in figure 10. Since the typical overlap is associated to the global maximum of g, the competition between the maximum at $q = 0$ and the maximum at $q > 0$ originates the jump in q_t, which takes place at the energy density where the two maxima have precisely the same height. The situation for non-zero h is more complicated. The correlations induced by the magnetic field destroy the region

of self-averageness of $\mathcal{N}(\epsilon)$. Interestingly, for a given $h > 0$ there is value of the energy density for which the typical overlap is minimal. For $p = 3$ the effect of the magnetic field is to decrease the size of the jump in q_t till it disappears altogether for $h \approx 0.29$. The results for $p > 3$ are qualitatively similar to those for $p = 3$. We mention only that the larger p, the larger the value of ϵ at which the discontinuity occurs, and the larger the value of h at which it disappears. Unfortunately, the enormous difficulty of solving the system of five coupled equations prevents a more systematic analysis of these discontinuities.

5 Conclusion

The analytical investigation of the statistical structure of the energy landscape of the p-spin Ising model presented in this paper is of interest from the viewpoint of the traditional statistical mechanics of disordered systems [7, 17, 18, 19] as well as from the perspective of the study of adaptive walks in rugged fitness landscapes [5, 11, 20]. Besides extending the calculation of the average number of optima to general p and non-zero magnetic field, we have focused on the characterization of the typical overlap q_t between pairs of identical optima. Interestingly, the dependence of q_t on the energy density ϵ is reminiscent of the dependence of the thermodynamic order parameter on the temperature T [12, 13]. We must note, however, that there is no relation between T and ϵ since $\ln \mathcal{N}(\epsilon)$ is not the entropy of the spin system. The quite complex effect of the magnetic field on the statistical properties of the energy optima motivates a more detailed study of the thermodynamics of the p-spin model for non-zero h. In fact, even the unambitious analysis of the first moment $\langle \mathcal{N}(\epsilon) \rangle$ has unveiled an interesting interplay between h and p that lead to a discontinuity in the typical energy density of the optima. Moreover, we have found that the magnetic field decreases the size of the jump in the typical overlap q_t that occurs for $p > 2$. It would be interesting to investigate whether a similar effect occurs for the thermodynamic order parameter as well, which might lead, eventually, to a continuous phase transition.

To conclude, we must mention that the calculations presented in this paper are free of all the mathematical subtleties that permeate the replica analyses of the infinite range Ising spin glass [9, 10]. Thus our results present a reliable account of the statistical properties of the p-spin energy landscape which, though may have little relevance to the thermodynamics of the model, are of considerable interest to the characterization of the fixed points (metastable states) of adaptive walks (zero-temperature Monte Carlo dynamics) on that landscape.

Acknowledgments This work was supported in part by Conselho Nacional de Desenvolvimento Científico e Tecnológico (CNPq). VMO holds a FAPESP fellowship.

References

[1] Kauffman S A 1993 *The Origins of Order* (Oxford University Press, Oxford)

[2] Dennet D C 1995 *Darwin's Dangerous Idea* (Simon & Schuster, NY)

[3] Kauffman S A and Levin S 1987 *J. Theor. Biol.* **128** 11

[4] Weinberger E D 1991 *Phys. Rev. A* **44** 6399

[5] Amitrano C, Peliti L and Saber M 1989 *J. Mol. Evol.* **29** 513

[6] Derrida B 1981 *Phys. Rev. B* **24** 2613

[7] Gross D J and Mezard M 1984 *Nuc. Phys. B* **240** 431

[8] Sherrington D and Kirkpatrick S 1975 *Phys. Rev. Lett.* **35** 1972

[9] Binder K and Young A P 1986 *Rev. Mod. Phys.* **58** 801

[10] Mezard M, Parisi G and Virasoro M A 1987 *Spin Glass Theory and Beyond* (Singapore: World Scientific)

[11] Weinberger E D and Stadler P F 1993 *J. Theor. Biol.* **163** 255

[12] Gardner E 1985 *Nuc. Phys. B* **257** 747

[13] Stariolo D A 1990 *Physica A* **166** 6229

[14] Thouless D J, Anderson P W and Palmer R G 1977 *Phil. Mag.* **35** 593

[15] Bray A J and M A Moore 1980 *J. Phys. C: Solid St. Phys.* **13** L469

[16] Rieger H 1992 *Phys. Rev. B* **46** 14655

[17] Tanaka F and Edwards S F 1980 *J. Phys. F: Met. Phys.* **13** 2769

[18] Roberts S A 1981 *J. Phys. C: Solid St. Phys.* **14** 3015

[19] Dean D S 1994 *J. Phys. A: Math. Gen.* **27** L899

[20] Stadler P F and Krakhofer B 1996 *Rev. Mex. Fis.* **42** 355

Figure captions

Fig. 1 The exponent f in $\langle \mathcal{N}(\epsilon) \rangle = \mathrm{e}^{fN}$ as a function of the energy density ϵ for $p = 2$ and $h = 0$, 0.5, 1.0, and 1.5.

Fig. 2 The typical energy density ϵ_t of the local optima as a function of h for (from top to bottom) $p = 2$ to $p = 10$. For $p \to \infty$ we find $\epsilon_t \to 0$. The dashed straight line is $\epsilon_t = -h$.

Fig. 3 The exponent f_t in the expression for the average number of optima $\langle \mathcal{N}(\epsilon_t) \rangle = \mathrm{e}^{f_t N}$ as a function of h for (from bottom to top) $p = 2$ to $p = 10$. For $p \to \infty$ we find $f_t \to \ln 2$.

Fig. 4 The lower bound ϵ_0 to the ground state energy density as a function of h for (from bottom to top) $p = 2$, 3, 4, and ∞. The dashed straight line is $\epsilon_0 = -h$.

Fig. 5 The exponent g_t in the expression for the average number of pairs of identical optima $\langle \mathcal{M}(\epsilon_t, q) \rangle = \mathrm{e}^{g_t N}$ as a function of q for $p = 7$ and (from top to bottom) $h = 0$, 1, 2, 2.5, 3, 3.3, 3.6, 3.8, 4 and 4.2.

Fig. 6 The typical value of the energy density of a pair of identical optima as a function of the overlap q for $p = 7$ and (from bottom to top) $h = 0$, 1, 2, 2.5, 3, 3.3, 3.6, 3.8, 4 and 4.2.

Fig. 7 The typical value of the overlap between pair of identical optima as a function of h for (from left to right) $p = 2$ to $p = 8$.

Fig. 8 The typical value of the overlap between pair of identical optima as a function of their energy density for $p = 2$ and $h = 0$, 0.5, 1.0, and 1.5. The marked points correspond to $f^{(2)} = 0$.

Fig. 9 Same as figure 8 but for $p = 3$, and $h = 0$, 0.27, 0.5, 1.0, and 1.5.

Fig. 10 The exponent g in the expression for the average number of pairs of identical optima $\langle \mathcal{M}(\epsilon, q) \rangle = \mathrm{e}^{gN}$ as a function of q for $p = 3$, $h = 0$, and (from top to bottom) $\epsilon = -0.73$, -0.75, -0.77, -0.79, and -0.81.

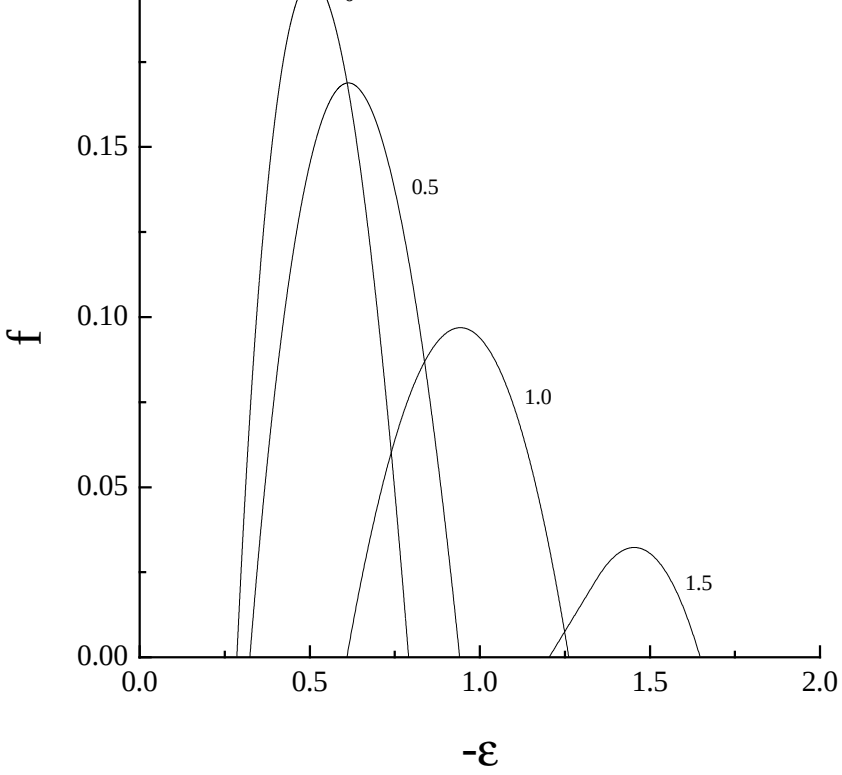

Figure 1

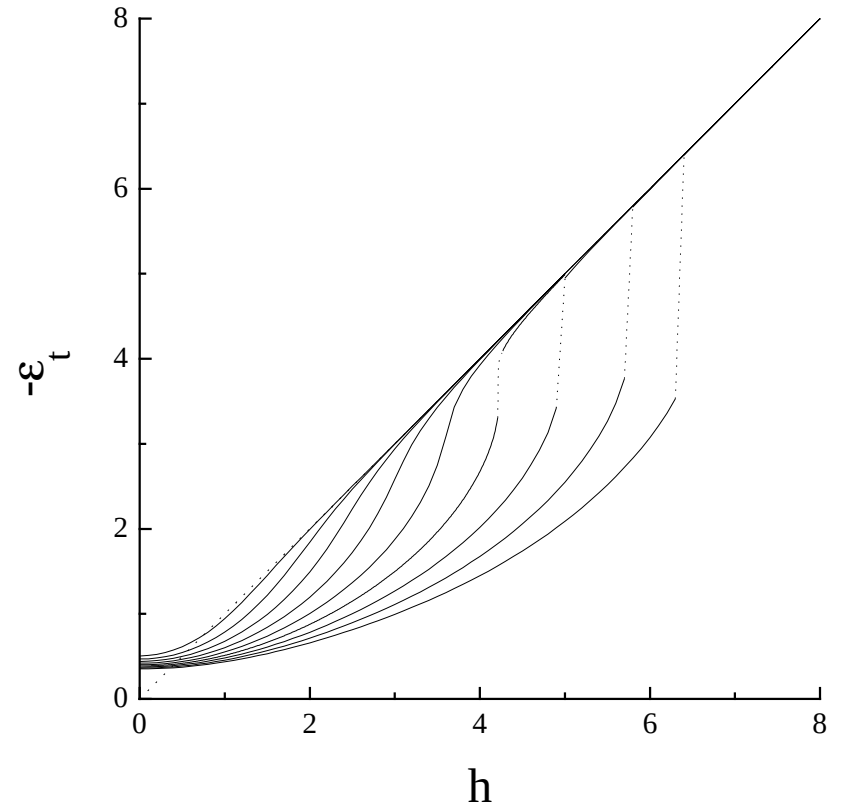

Figure 2

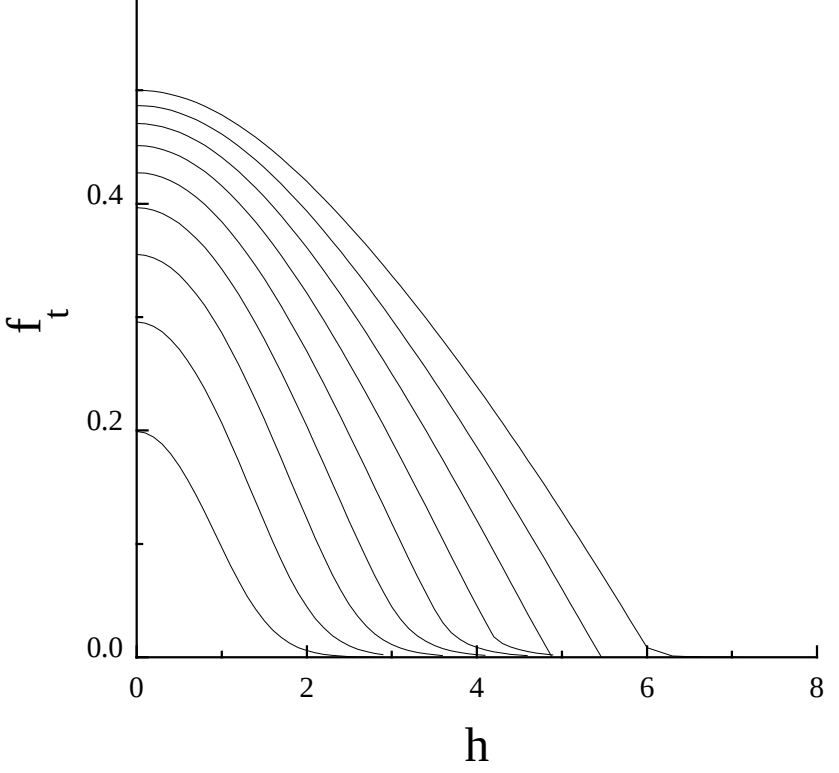

Figure 3

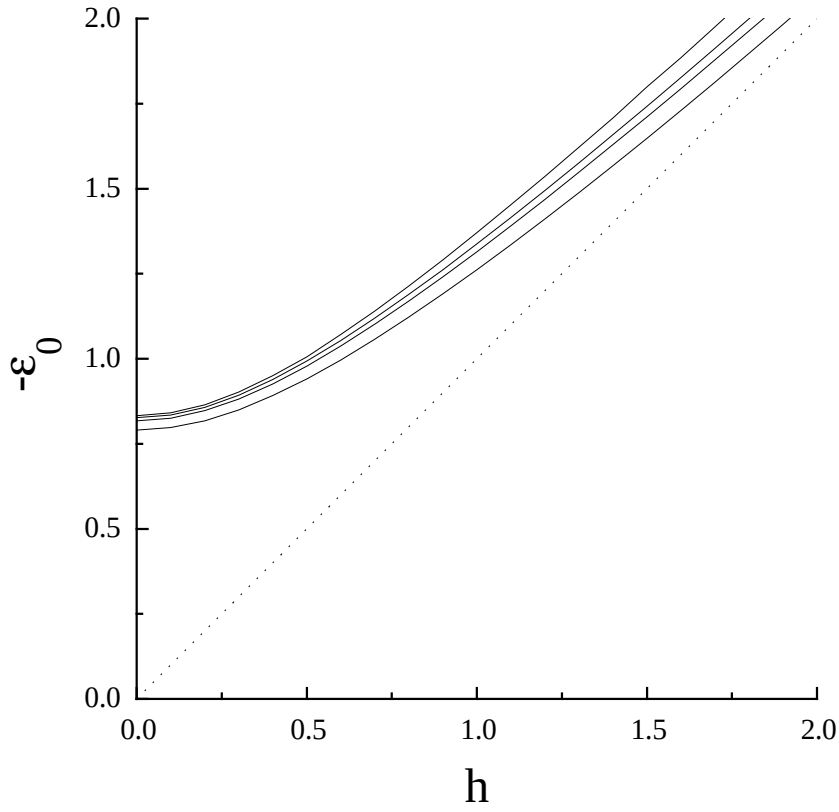

Figure 4

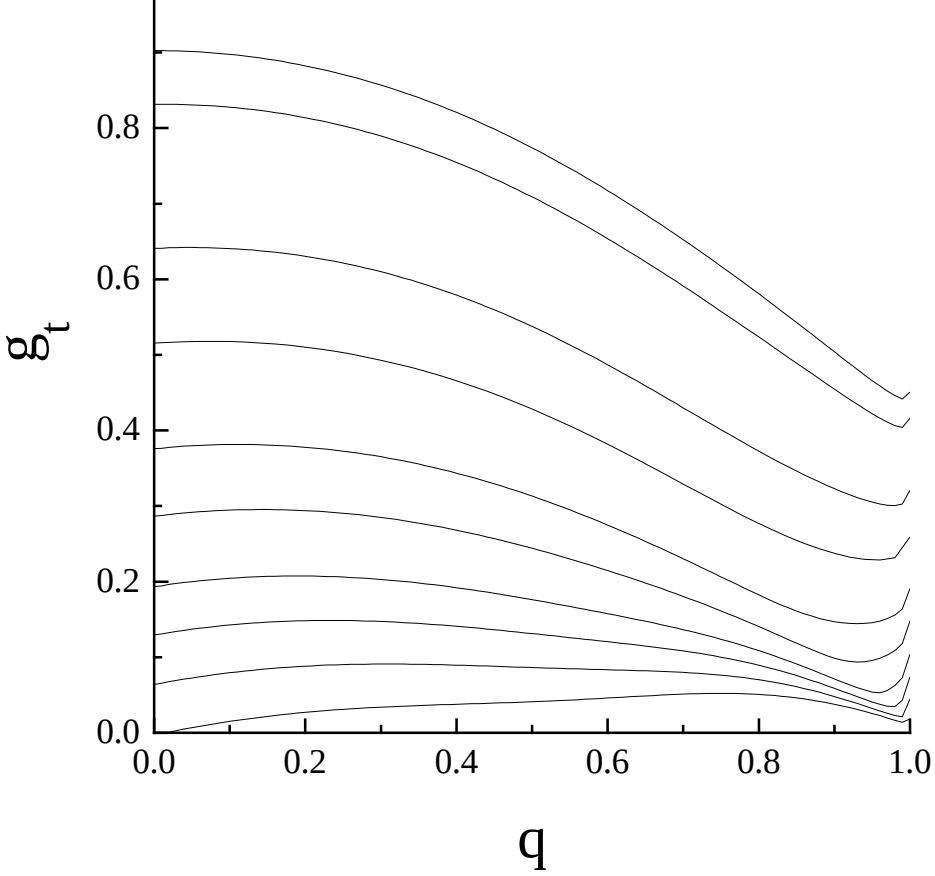

Figure 5

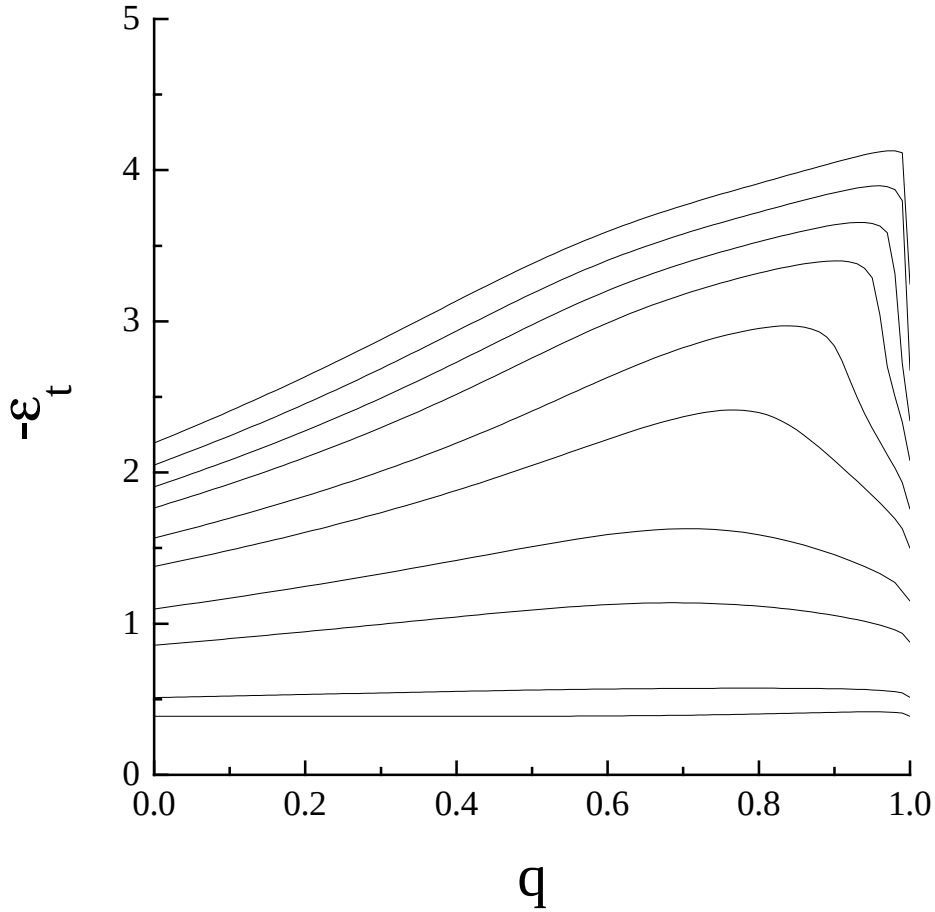

Figure 6

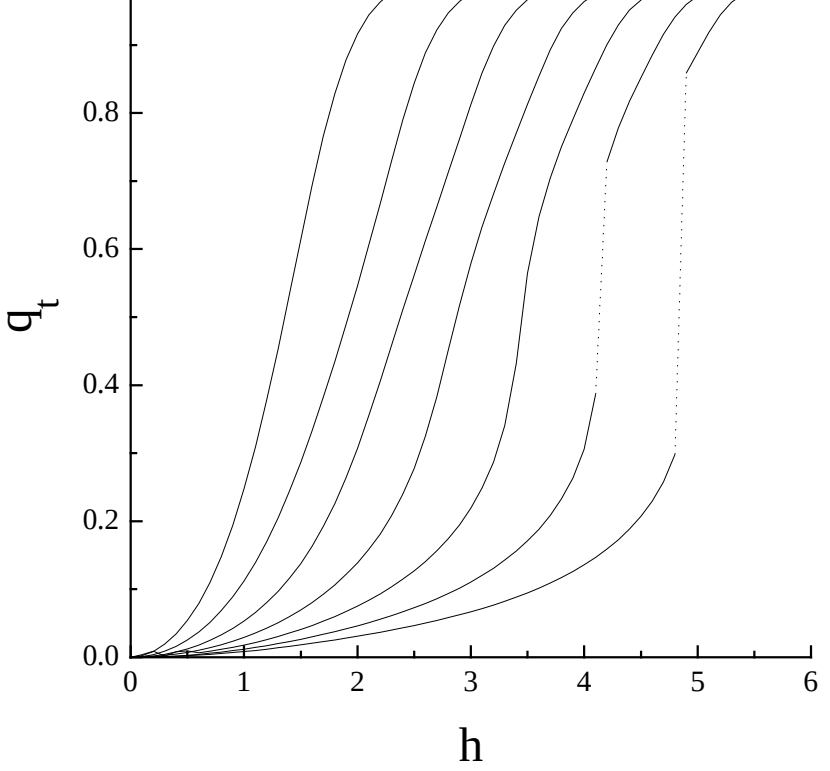

Figure 7

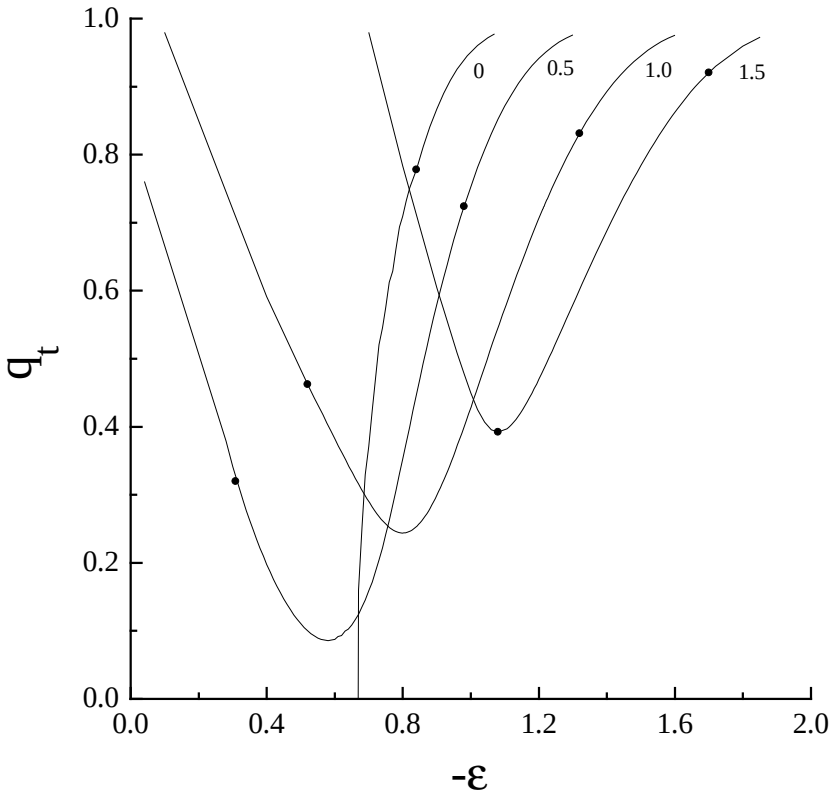

Figure 8

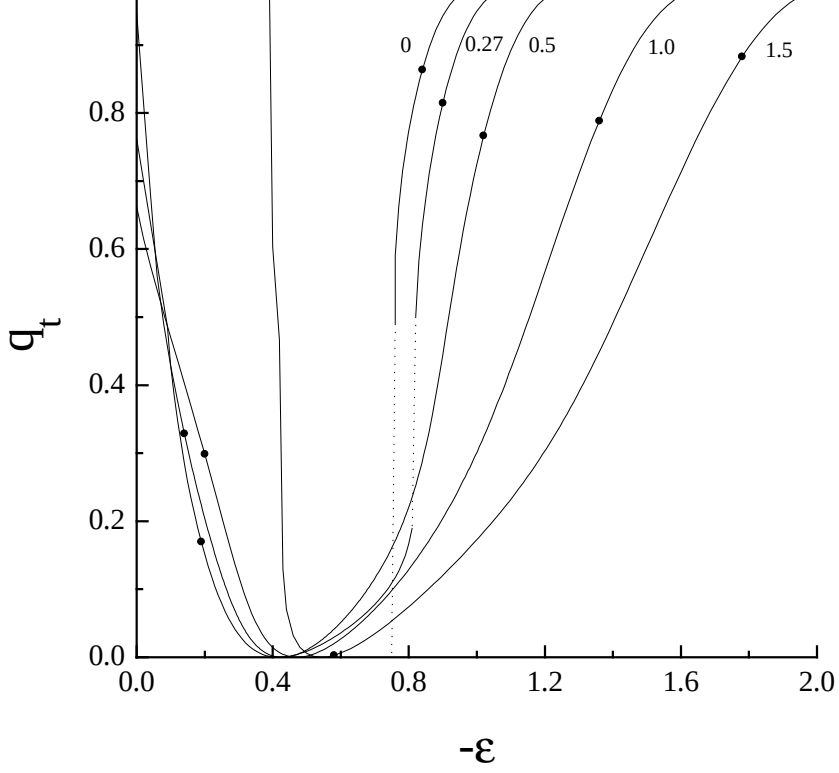

Figure 9

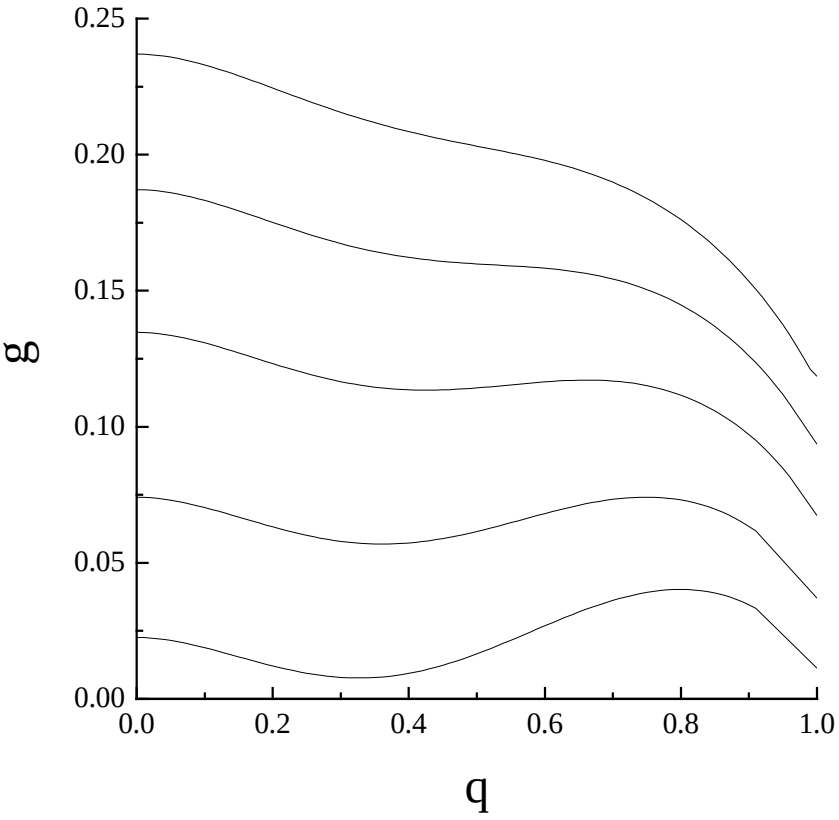

Figure 10